Physics Letters A 380 (2016) 3640–3644

Contents lists available at ScienceDirect

Physics Letters A

www.elsevier.com/locate/pla

Signature of triply excited Li-like V states in ion–solid collisions

Gaurav Sharma [a], K. Haris [b], G. Singh [a], B. Kumar [c], S. Karmakar [d], N.K. Puri [a], Adya P. Mishra [e], Pravin Kumar [f], T. Nandi [f,*]

[a] Delhi Technological University, DTU, Delhi 110042, India
[b] Dept. of Physics, Aligarh Muslim University, Aligarh 2022002, India
[c] Jai Prakash Vishsvidyalaya, Chapra, Bihar 841301, India
[d] Lalbaba College, 117 G.T. Road, Belur Math, Howrah 711202, India
[e] Atomic and Molecular Physics Division, Bhabha Atomic Research Centre, Trombay, Mumbai 400 085, India
[f] Inter University Accelerator Centre, IUAC, New Delhi 110067, India

ARTICLE INFO

Article history:
Received 31 May 2016
Received in revised form 12 August 2016
Accepted 13 August 2016
Available online 31 August 2016
Communicated by V.A. Markel

Keywords:
Beam-foil interaction
Triply excited states
Autoionizing Rydberg states
Double autoionization

ABSTRACT

The transitions originating from triply excited, doubly autoionizing states of Li-like V formed in beam-foil experiments detected within a set of blended spectroscopic profiles have been assigned tentatively by the Hartree–Fock calculations including relativistic corrections and multi-configuration interactions as perturbations. The x-ray decay channels from the triply excited states such as $3p^3\ {}^4S$, $2p^2np\ {}^4S$ ($n \sim 12$) through radiative transitions to the ground state via two or more steps have been observed.

1. Introduction

The simplest four-body Coulomb interactions are studied by the atomic Li and Li-like ions. These systems exhibit distinct electron–electron correlation effects when all three electrons are excited forming the triply-excited states. These states mostly lie above the second ionization limit, and decay normally via autoionization. Sometimes the triply excited states is formed with such total spin, parity and angular momentum that it cannot find any suitable lower states to autoionize and thus the states remain metastable against autoionization. Thus, even though the $2p^3\ {}^4S^\circ$ state lies above the second ionization limit, the dominant decay is the radiative dipole allowed transition to the $1s2p^2\ {}^4P$ state in Li-like ions [1]. Nevertheless, the other states of $2p^3$ such as $2p^3\ {}^2D^\circ$, ${}^2P^\circ$ are autoionization allowed; and besides the single autoionization, the double autoionization becomes possible. Consequently, a double autoionizing level can decay either by one-step double autoionization or two-step sequential single-autoionization. Recently, both types of autoionization processes have been observed experimentally in Li atom [2,3]. The one-step double autoionization channel is usually much slower compared to two-step sequential single-autoionization and thereby it is rare. Whatsoever, the theoretical study of triply excited, and the double autoionizing states is challenging as the absolute ionization strengths are difficult to predict [4].

Various techniques such as the beam–foil spectroscopy [5–10], the electron and the photon impact [1,11,12] and the theoretical investigations [13–15] are available to study the above mentioned exotic atomic systems for the understanding of the triply excited systems. The impact of highly charged ions which can lead to a different excitation mechanism in this exotic systems is not studied in great detail [1,16–18]. The interactions between the highly charged ions and the solid surfaces [18,19] yields to the hollow states like the triply excited states in Li-like ions. Sometimes this interaction allow one of the excited electron in the triply excited states lie in the high orbit and they can be named as the triply excited Rydberg states or the double-autoionizing Rydberg states. Nevertheless, the impact of fast energetic ions with the solid surface is necessary to create varieties of the triply excited Li-like states in high Z systems.

Resolving the triply excited states from other excited states of the projectile ions is necessary for absolute intensity measurements and hence determination of the branching ratios. Very often the lifetime of triply excited states in highly charged ions is small and thus comparable to that for the singly and doubly excited states, which makes the measurement more challenging. Therefore, the standard beam–foil time-of-flight technique; has remained limited to the Li-like carbon [5–10,12] for studying the

* Corresponding author.
E-mail addresses: nanditapan@gmail.com, nandi@iuac.res.in (T. Nandi).

http://dx.doi.org/10.1016/j.physleta.2016.08.026
0375-9601/

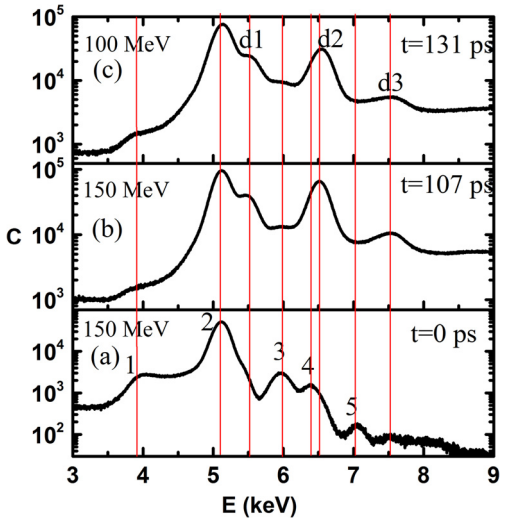

Fig. 1. X-ray spectra recorded after an energetic beam of V^{11+} emerges out of 80 μg/cm^2 thick carbon foil: (a) Prompt x-ray spectrum with the beam energy 150 MeV, (b) and (c) represent the delayed spectra at the beam energy 150 and 100 MeV, respectively.

four body systems. The radiative transitions from the triply excited states in the heavier systems in the beam–foil interactions can be recorded, in principle, with a suitable technique. We have made use of the high-efficiency solid-state detector to record the prompt and the delayed x-ray spectra from the double autoionizing states of Li-like V ions, provided they are metastable against autoionization. Otherwise, they follow two-step single autoionization and no x-ray emissions are possible. The observed blended profiles are assigned tentatively by the Hartree–Fock calculations using the COWAN code [20], where single configuration calculation approach is used and both, relativistic corrections and configuration interactions, are treated as perturbations. In this paper, we discuss a sort of the evidence for several double autoionizing states as well as double-autoionizing Rydberg states of Li-like V decaying through the radiative channels.

2. Experimental details

The experiments were performed using the 15 UD tandem Pelletron accelerator at IUAC, New Delhi, India. A beam of $^{51}_{23}V^{11+}$, having energy of 100 and 150 MeV was passed through 80 μg/cm^2 thick carbon foil to produce the excited states in highly charged ions. The targets were placed in a small vacuum chamber maintained at a pressure better than 1×10^{-6} Torr. The carbon foil was mounted on either surface of an aluminum ladder so that the distance between two positions remained to be 2.55 mm. A germanium ultralow energy detector (GUL0035, Canberra Inc., with 25 μm thick beryllium entrance window, resolution ∼150 eV at 5.9 keV), was placed in perpendicular geometry at 50 mm away from the beam axis in such a way that it views the beam just after the back surface of the foil holder. Thus, when the foil is mounted on the front surface of the holder, the x-ray spectra are recorded at delay times about 100–140 ps depending upon the beam energy. Whereas if it is mounted on back side of the holder, the recorded spectra corresponds to time $t \to 0$ with respect to the center of the collimator placed in front of the detector. The observed x-ray spectra were calibrated with a ^{241}Am source.

3. Results and discussion

The prompt and the delayed x-ray spectra of the foil excited $^{51}_{23}V^{11+}$ ions are shown in Fig. 1. The spectrum taken at $t \to 0$ differs from the delayed spectra. The most prominent line appears at 5.12 keV. A few lines in the prompt spectra disappear either completely or decrease in intensity with the delay. Besides, we see a peculiar structure in delayed spectra. Certain peaks become more prominent with the delay such as the lines at 5.4, 6.5, and 7.5 keV marked as d1, d2, and d3. Such kind of features has been observed recently with H-like ions of projectile [21–23] and projectile-like ions [24] owing to the formation of circular Rydberg states. The excited states corresponding to the maximum orbital quantum number (l_{max}) as well as magnetic quantum numbers ($|m|$) for a particular principal quantum number (n) satisfying the relation $l_{max} = |m| = n - 1$ have exactly a circular path and are called the circular Rydberg states [25], which decay via the resonance state through the cascading chain leading to the E2 transitions. Therefore, the delayed transitions observed in present study are expected to originate from the circular Rydberg states. The circular Rydberg states can be observed either through the resonances appearing on the lifetime decay curve of a certain metastable state [22] or the current technique involving the prompt and the delayed measurements. If the time-of-flight is selective, the resonance will be missing in the measurement and one measures only the decay of the metastable level [26].

The lines in prompt spectra which disappear or decay with the delay are labeled as 1, 2, 3, 4 and 5. The transitions assigned to these lines are given in Table 1. The peak energies of the lines observed in all the three spectra of Fig. 1 as given in Table 1 are the average value with the error of $\sim \pm 50$ eV. The most prominent line observed at 5.12 keV belongs to the K_α-lines in the V^{q+} ions, where q is the charge state of the outgoing ions. The equilibrium charge state distribution of the V ions can be estimated from the code ETACHA [27]. The charge state fractions obtained for 17+ to 23+ states producing with the impact of the 100 MeV V^{11+} beam are 14, 25, 28, 18, 5, 0.17, and 0.0017%, respectively. Whereas, the same for the 150 MeV V^{11+} projectiles are 2, 10, 25, 35, 22, 2, and 0.067%, respectively. Since, the peak remains to be most prominent even with the delays, the line must be arising predominantly from the forbidden transitions including $1s2p\ ^3P_2$–$1s^2\ ^1S_0$ in He-like V and the $1s2s2p\ ^4P_{5/2}$–$1s^22s\ ^2S_{1/2}$ line in Li-like V ion [28]. Though the energy of the transition $1s2s\ ^3S_1$–$1s^2\ ^1S_0$ in He-like V lies within the peak profile, but its presence can be ignored due to its low transition probability (6.07×10^7/sec) compared to the other two lines (see Table 1). One point is worth noting here that the $1s2s2p\ ^4P_{5/2}$ level lies above the first ionization potential, and thereby it may decay to all the $1s^2ns\ ^2S_{1/2}$ levels for $n = 2, 3, 4, 5$, etc. The broad structure observed around 4 keV (line 1) corresponds to the transitions $1s2s2p\ ^4P_{5/2}$–$1s^2ns\ ^2S_{1/2}$ ($n = 3$–5). The individual lines are quite close to each other, but the calculated transition probability of the peak (shown in Table 1) suggests a bit higher intensity for the $1s2s2p\ ^4P_{5/2}$–$1s^23s\ ^2S_{1/2}$ transition. The contribution from the transitions $1s2s2p\ ^4P_{3/2,1/2}$–$1s^2ns\ ^2S_{1/2}$ ($n = 3$–5) comes at $t \to 0$ and also in the delayed spectra due to their long lifetime (123 ± 13 ps [28]) as seen in Fig. 1. Further, the He-like transitions $1s4p$–$2s^2$ and $2p^2$–$1s5s$ lie at this energy domain and hence the contribution arising from them cannot be fully ruled out. In addition, the β transition of the line $1s2s2p\ ^4P_{5/2}$–$1s^2ns\ ^2S_{1/2}$ i.e., $1s2s3p\ ^4P_{5/2}$–$1s^22s\ ^2S_{1/2}$ corresponds to the observed line at 5.99 keV (line 3) due to its quite close energy and a large lifetime 389 ps. Since this line almost disappears with the delay, it must be predominantly originating from a much faster transition such as $1s3p^2\ ^2S$–$1s^23p\ ^2P$. The energy of the transition (6.10 keV) is quite close to the measured value and the upper level lifetime is also as short as 9.4 fs. Though $1s3p^2\ ^2P$, ^2D, ^4P–$1s^23p\ ^2P$ and $1s3p\ ^3P_{1,2}$–$1s^2\ ^1S_0$ lines are also close to this energy, but their lifetimes are 44 ps, 38 ps, 0.2 ps, and 0.23 ps, respectively. The line remains present with the delay and thus, the contribution from these transition as well as $1s2s3p\ ^4P_{5/2}$–$1s^2ns\ ^2S_{1/2}$ can-